



Volume XXIII 2020

ISSUE no.2

MBNA Publishing House Constanta 2020



Scientific Bulletin of Naval Academy

SBNA PAPER • **OPEN ACCESS**

Improving resistance properties of high-speed ships

To cite this article: K.Turgut Gürsel, Mesut Taner, Deniz Ünsalan, Gökdeniz Neşer and Erkin Altunsaray, *Scientific Bulletin of Naval Academy*, Vol. XXIII 2020, pg.8-18.

Available online at www.anmb.ro

ISSN: 2392-8956; ISSN-L: 1454-864X

doi: 10.21279/1454-864X-20-I2-001

SBNA© 2020. This work is licensed under the CC BY-NC-SA 4.0 License

Improving Resistance Properties of High-Speed Ships

K.Turgut Gürsel, Mesut Taner, Deniz Ünsalan, Gökdeniz Neşer, Erkin Altunsaray

Dokuz Eylül University –Institute of Marine Sciences and Technology – Department of Naval Architect – Bakü Bulvarı, No: 100, İnciraltı – 35340 İzmir

Corresponding author: turgut.gursel@deu.edu.tr

Abstract. Sustainable engineering solutions facilitate and/or force the use of energy more efficiently and, thus, reducing the carbon emission to the atmosphere. This study is related to improving resistance properties of ships, especially in the high speed range, in which they consume large amount of fuels. In this investigation, the model of the Kriso Container Ship (KCS) was taken as the basis to be studied and she was hydrodynamically analysed through the commercial software STAR-CCM+. After the successful validation of the results obtained in these computational fluid dynamics (CFD) analyses by those of the experiments of this model published in [1], the simulations carried out on the models equipped with stern flaps and a combination of stern flaps and interceptors for reducing resistance of the models, were performed in the same manner using the same software. Then the results obtained in all analyses were discussed by comparing those with the test ones.

1. Introduction

Within the scope of sustainable engineering solutions, the number of studies dealing with the use of energy more efficiently and thus reducing the carbon emission to the atmosphere has been increasing significantly in recent years. In this regard, optimization of ship forms, reducing their total resistance and increasing propulsion efficiency, thus reducing their fuel consumption and achieving the targeted cruising speeds with less engine power requirements are among the main tasks of naval architects, which agree the guidelines of “green technologies”.

Due to low investment and operating costs, one of the most important design factors for both small craft and larger ships is to reduce the hull resistance force and to increase the related thrust force, i.e. increasing the propulsive efficiency. Furthermore, accurate prediction of the hull resistance of a marine vehicle is the most fundamental factor for determining a specific range of power requirements and hence the operation route of the vehicle. As a solution to both above-mentioned reasons, accurate computational fluid dynamics (CFD) analyses of models are of great importance.

In general, reasons submerged in a fluid are exposed to viscous drag that can be resolved to two components, i.e. the viscous pressure and frictional resistance components, both of them being a function of the Reynolds number. If the moving objects are at motion on the free fluid surface, these objects additionally experience wave resistance being a function of the Froude number. Thus, both small craft and big ships must possess proper hydrodynamic form and surface characteristics for reducing their

frictional and viscous pressure resistance as well as wave resistance component, all depending on vehicle speed.

The main source of wave resistance is pressure changes on the surface and inside of the fluid. Due to the basic principles of fluid mechanics, a positive pressure field on the bow of marine vessels and a negative pressure region in front of their propellers in forward motion develop which usually impair propulsion properties and causes a trimming by the stern of ships in high-speeds, which increases its total resistance. However, this state is partially improved by appropriate selection of the longitudinal centre of buoyancy and by conveniently forming the bow and the stern of the marine vehicle. Additionally, large ships can often cruise with a certain stern trim due to the further improvement of the propulsion characteristics. Except those, reducing this negative pressure field in front of the propeller through local turbulence increase can improve propulsive efficiency and mitigate the height of stern wave, which contributes to the reduction of ship resistance. This reduction can be achieved appendages as interceptors and stern flaps as well as trim tabs as seen in Figure 1.

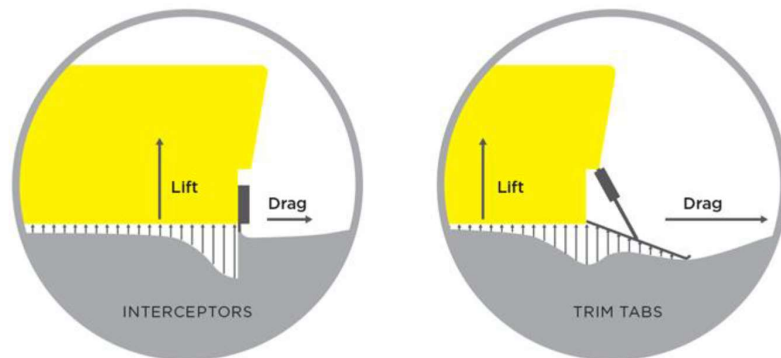


Figure 1. Installation and effect of stern appendages: Interceptor (left) and trim tabs (right) [2]

In this special field, Zou et al (2019) investigated the coupled effects of flaps and stepped hulls. Therefore, experimental and numerical simulation methods were carried out in [3] to explore the influence of the flap mounting angle coupled with steps. Their test results indicated that the low speed resistance performance was improved and the porpoising critical speed was delayed with a slight resistance penalty when the mounting angle increased [3].

Uithof et al (2016) declared in [4] that the pitch motion and the added resistance of the ship due to waves was reduced effectively by applying a Hull Vane® on larger vessels. Moreover, a resistance reduction of only 10.1% was found at 17 knots, increasing to 15.5% at 21 knots during earlier tests in flat water.

In the study of [5], Uithof et al (2017) discussed a comparison between the Hull Vane® and other trim correction methods such as interceptors, trim wedges and ballasting. The results show that the Hull Vane® effectively reduces the pitching motion and the added resistance in waves more than an interceptor.

Cumming et al (2006) explained in [6] that the addition of a suitable stern flap appendage can reduce fuel costs of the HALIFAX Class frigates from 5 to 10%, depending on the operational profile of the ship. Cusanelli (2002) stated the test results on RAMAGE in [7] that the stern flap reduced delivered power by 5-15%.

In the article of [8] with a systematic deployment of interceptors, Avcı and Barlas (2019) obtained a significant drag reduction between 1.50-11.30% within Froude number (Fr_n) range of 0.58-1.19 and observed a trim reduction of 1.60° up to 4.70°. Moreover, the other significant conclusion showed that the effect of the interceptors decreases from keel to chine for the same blade deployment heights.

Song et al (2018) reported in [9] that both the stern flaps and interceptors provide a drag reduction rate of the order of 3–9% in the Fr_n range of 0.334–0.584 in a deep-vee ship (Fig. 2). Resistance performance of the deep-vee ship equipped with stern flaps was better in the Fr_n range of 0.334–0.5; however, while the ship equipped with interceptors demonstrated better drag-reduction effect over $Fr_n=0.5$. They argued that a reasonable combination of stern flaps and interceptors causes significant improvement in the drag-reduction effect and trim optimization (Fig. 2).

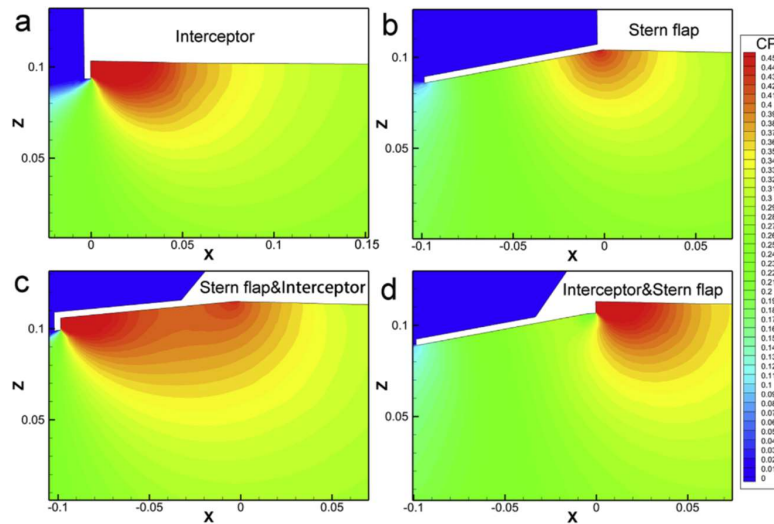


Figure 2. Comparison of high-pressure region at stern created by installation of stern appendages a) interceptor; (b) stern flap; (c) stern flap & interceptor (d) interceptor & stern flap [9]

In this regard, this study is aimed to perform a comprehensive computational fluid dynamics (CFD) analysis of the KCS model (Fig. 3) and the validation of the results obtained in these analyses with those of the experiments of this ship model published in [1] (Table 1). After demonstrating successful conformity of the simulations conducted using the commercial software STAR-CCM+, stern hull of the KCS Model I will be equipped with stern flaps and that of the KCS Model II with a combination of stern flaps and interceptors for increasing local pressure distribution which shall cause no significant resistance increase (Fig. 4). Then, CFD analyses will be carried out with varying these stern appendages, and subsequently the results obtained will be discussed.

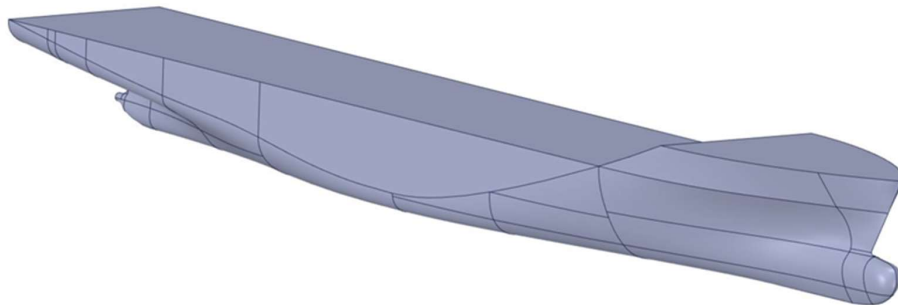


Figure 3. KCS ship model [10]

Table 1. Dimensions of the KCS ship and model [10]

	Ship	Model
Scale	1	31.599
L_{pp} (m)	230	7.2786
L_{wl} (m)	232.5	7.357
B_{wl} (m)	32.2	1.019
D (m)	19	0.6013
T (m)	10.8	0.3418
Displacement (m^3)	52,030	1.649

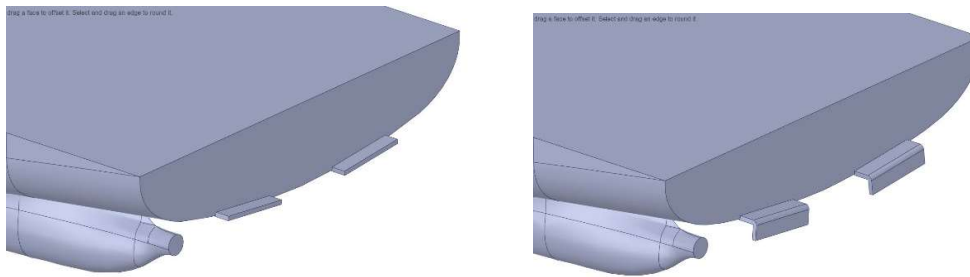


Figure 4. Applying appendages to the stern of the Model I and II equipped with stern flaps (left) and a combination of stern flaps and interceptors, respectively (right)

2. Materials and Method

The pressure difference in front of and behind a ship propeller as well the form and the wake zone of ships are the reasons that increase wave resistance and decrease propulsive efficiency of ships. Thus, equipping ships with a system such as stern flaps and/or a combination of stern flaps and interceptors can give hydrodynamically positive results as following reasons (Fig. 1-4):

- It reduces the pressure difference in the wake fluid zone around the propeller,
- enables weakening the wave formation and
- increases the turbulence formation in front of the propeller locally and, thus, increases fluid velocities in the wake zone.

In the preliminary study phase of the ship model, by means of taking into consideration an initial literature survey for high-speed ships and experiences gained from previous high-speed boat designs, when applying different appendages to high-speed ships, the following topics were investigated [1-10]:

- Possibility to lowering total resistance of ships,
- Low manufacturing costs,
- Low maintenance and operating costs.

Further, the KCS model equivalent to this published in [1] was modelled and analysed (Figs. 3-6). After the results obtained from the simulations had been validated with those of the physical towing tank tests of this KCS model (Fig. 6), numerical hydrodynamic analyses of the KCS Models I and II equipped with stern flaps and a combination of stern flaps and interceptors at the bottom parts of the stern, respectively, were performed to estimate model resistances at a service speed up to 2.196 m/s (Figs. 7-12). The chord length of the flaps and interceptors was varied in 5%, 7.5% and 10% of the

model draught T . Furthermore, it was found out that the increase in resistance was proportional to the second power of velocities, which was expected.

The aim was to be found out how these appendages and the variation of their chord length function. After analyzing the Models I and II in the same manner as the basic KCS model, it was determined that resistance values of the both Models equipped with stern flaps and a combination of stern flaps and interceptors with increased chord length of 5 % of T , were up to 4 % lower than those of the basic model (Fig. 11-12). This can result in significant fuel savings for the same service speeds or higher speeds with a smaller engine requirement.

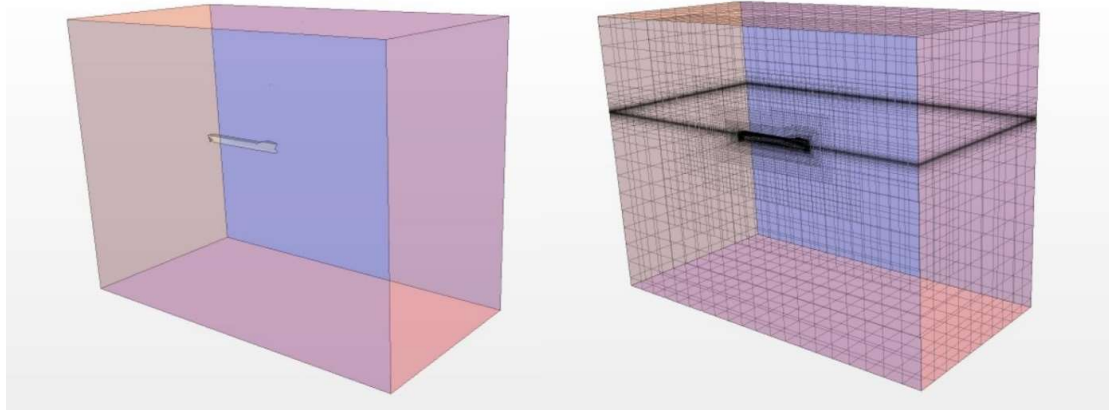


Figure 5. Domain of the model analysed in this study

Figure 3 indicates the model of the KCS while Figure 5 shows the domain of the system analysed. As can be seen in Figure 6, a good agreement between the results of the CFD analyses carried out in this study and the experiments performed in [1], was achieved. In all CFD analyses carried out, the turbulence modelling “ $k-\epsilon$ ” algorithm of the software STAR-CCM+ was applied [11]. The reason for the selection of this algorithm was that various forms of the $k-\epsilon$ model have been in use for a number of decades, and it has become the most widely and successfully used model for industrial applications (Equation 1 and 2).

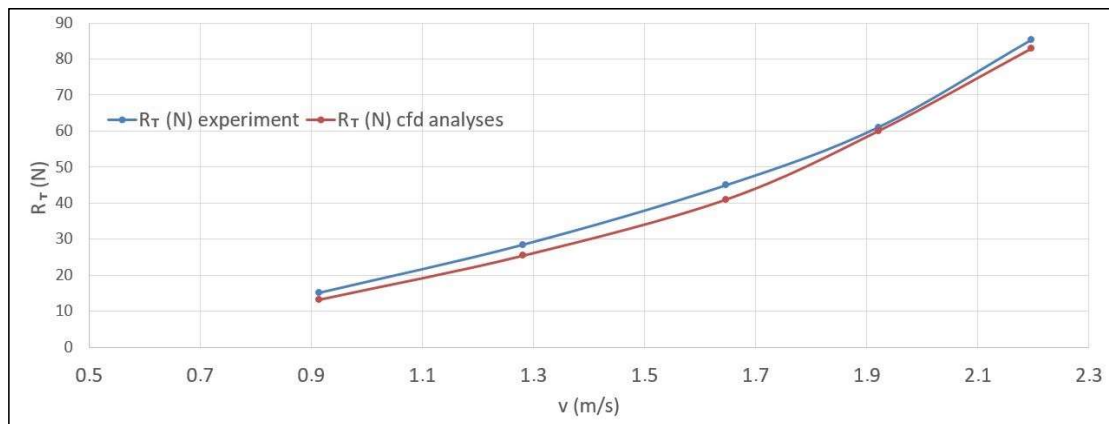


Figure 6. Total resistance values of the KCS model measured by the experiment in [1] and determined by CFD analyses in this study

The transport equations for the kinetic energy k and the turbulent dissipation rate ε used in $k-\varepsilon$ algorithm of the software STAR-CCM+, are:

$$\frac{\partial}{\partial t}(\rho k) + \nabla \cdot (\rho k \bar{\mathbf{v}}) = \nabla \cdot \left[\left(\mu + \frac{\mu_t}{\sigma_k} \right) \nabla k \right] + P_k - \rho(\varepsilon - \varepsilon_0) + S_k \quad (\text{Equation 1})$$

$$\frac{\partial}{\partial t}(\rho \varepsilon) + \nabla \cdot (\rho \varepsilon \bar{\mathbf{v}}) = \nabla \cdot \left[\left(\mu + \frac{\mu_t}{\sigma_\varepsilon} \right) \nabla \varepsilon \right] + \frac{1}{T_e} C_{\varepsilon 1} P_\varepsilon - C_{\varepsilon 2} f_2 \rho \left(\frac{\varepsilon}{T_e} - \frac{\varepsilon_0}{T_0} \right) + S_\varepsilon \quad (\text{Equation 2})$$

Where:

$\bar{\mathbf{v}}$ is the mean velocity,
 μ is the dynamic viscosity,
 σ_k , σ_ε , $C_{\varepsilon 1}$ and $C_{\varepsilon 2}$ are model coefficients,
 P_k and P_ε are production terms,
 f_2 is a damping function,
 S_k and S_ε are the user specified source terms,
 T_e is the large-eddy time scale.

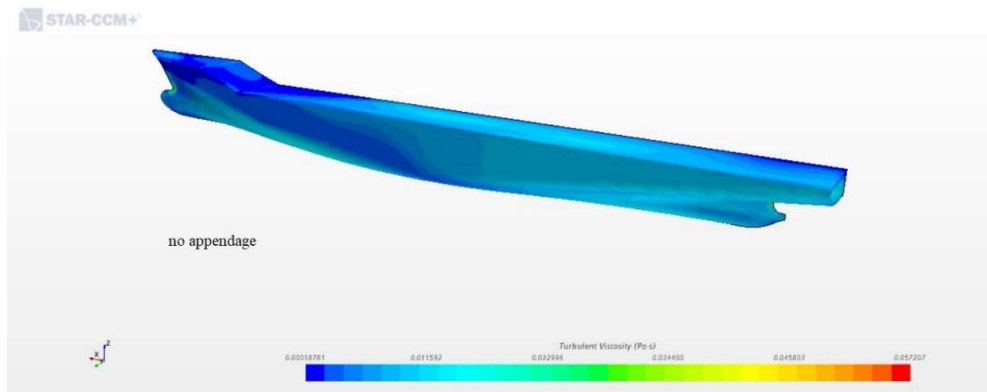


Figure 7. Turbulent viscosity alongside the original KCS model without any appendages at $v=2.196$ m/s.

As seen in Figures 7 and 8a,b-10a,b, turbulent viscosity distributions alongside the original KCS model and all of the other models equipped with stern flaps and a combination of stern flaps & interceptors with variable chord lengths at $v=2.196$ m/s, appear to be very suitable.

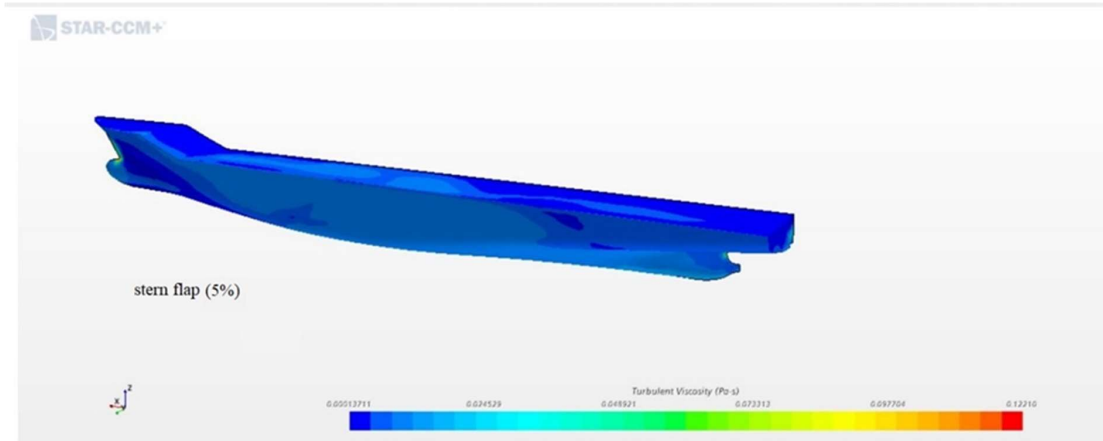


Figure 8a. Turbulent viscosity alongside the models equipped with stern flaps with chord length of 5% T at $v=2.196$ m/s.

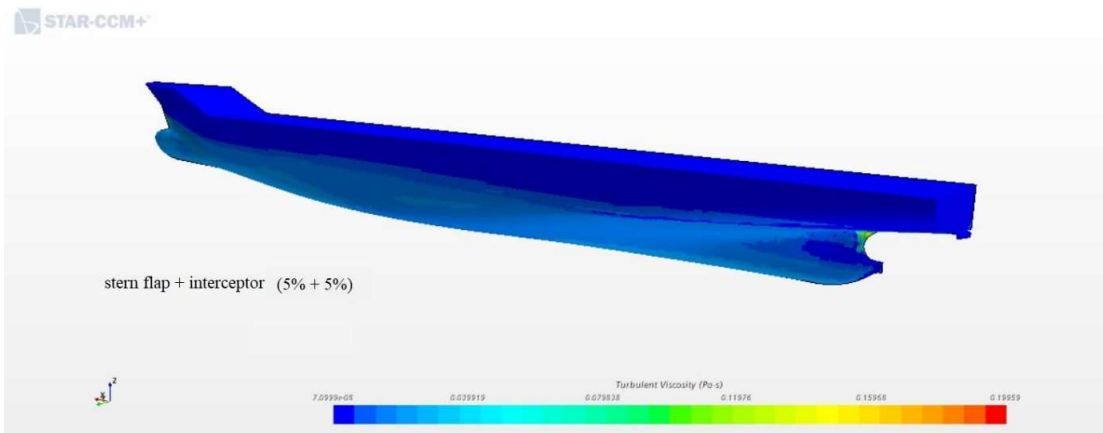


Figure 8b. Turbulent viscosity alongside the models equipped with a combination of stern flaps & interceptors with chord length of 5% T at $v=2.196$ m/s.

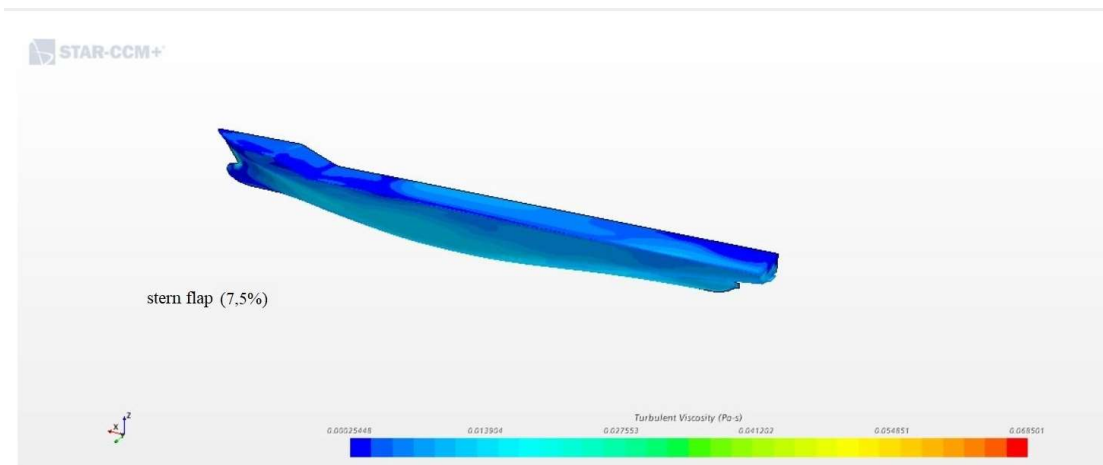


Figure 9a. Turbulent viscosity alongside the models equipped with stern flaps with chord length of 7.5% T at $v=2.196$ m/s

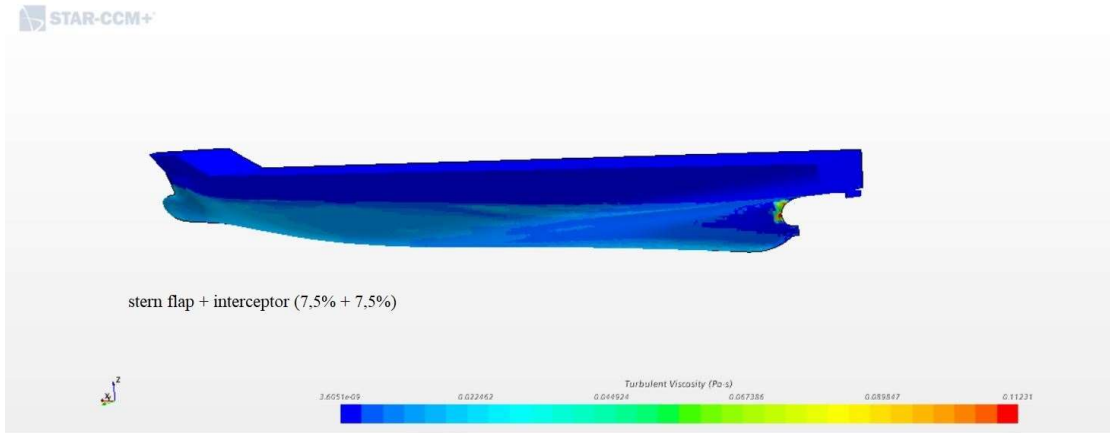


Figure 9b. Turbulent viscosity alongside the models equipped with a combination of stern flaps & interceptors with chord length of 7.5% T at $v=2.196$ m/s.

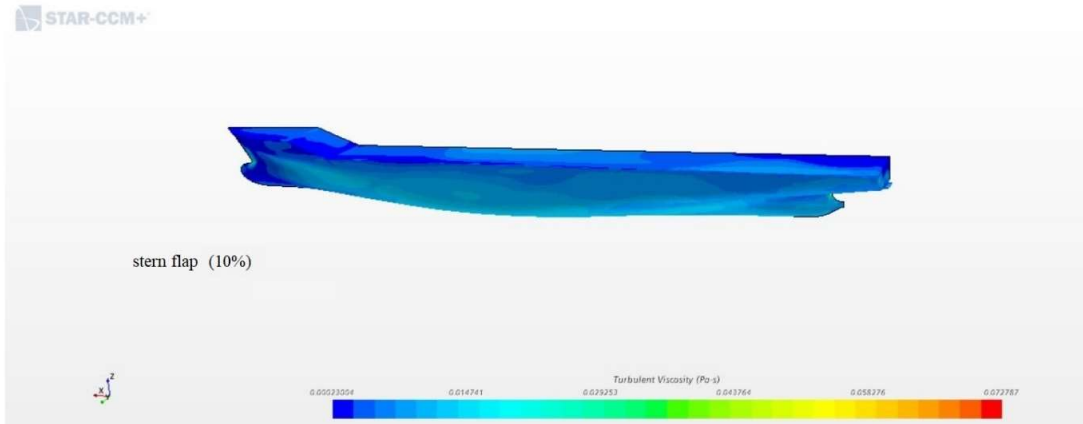


Figure 10a. Turbulent viscosity alongside the models equipped with stern flap with chord length of 10% T at $v=2.196$ m/s.

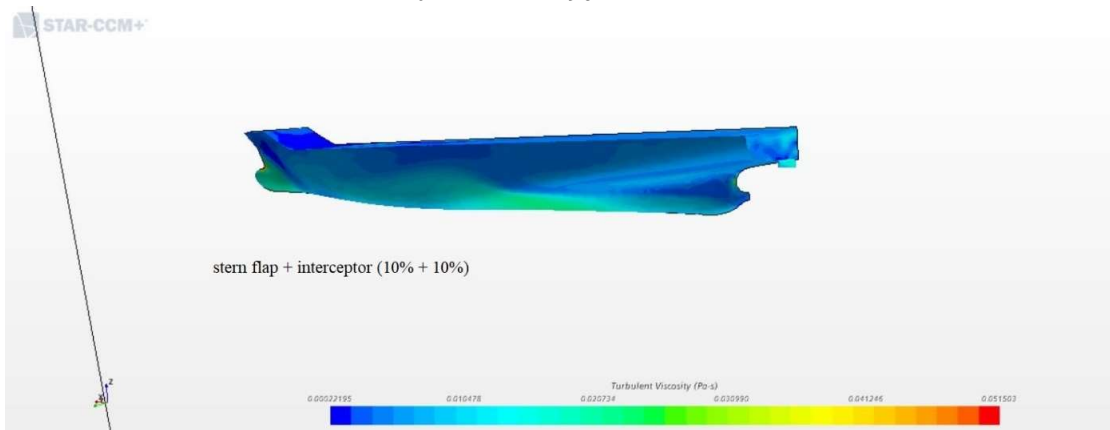


Figure 10b. Turbulent viscosity alongside the models equipped with a combination of stern flaps & interceptors with chord length of 10% T at $v=2.196$ m/s.

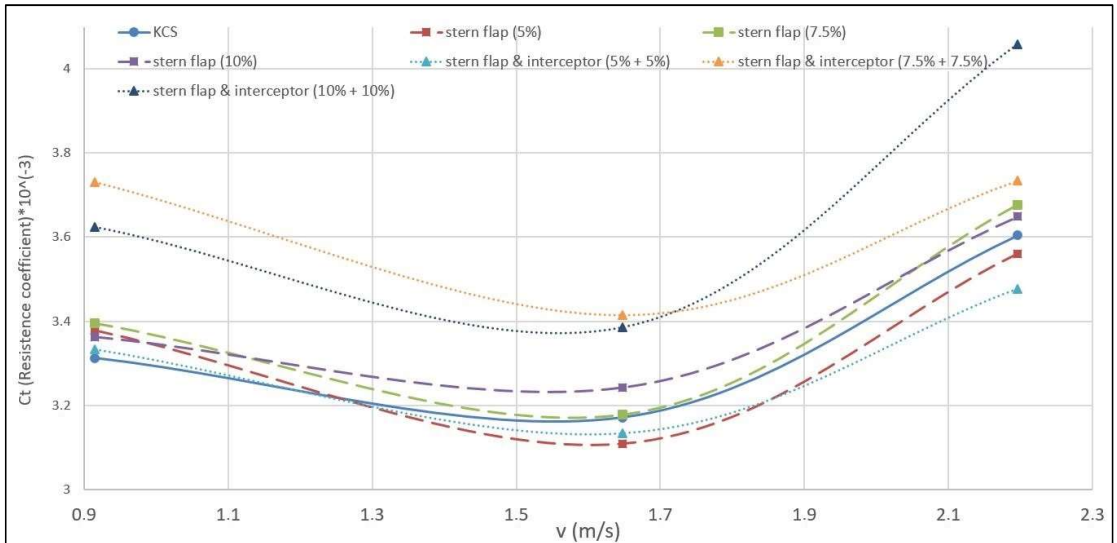


Figure 11. Total resistance coefficient values (C_T) of all models estimated at speed up to 2.196 m/s

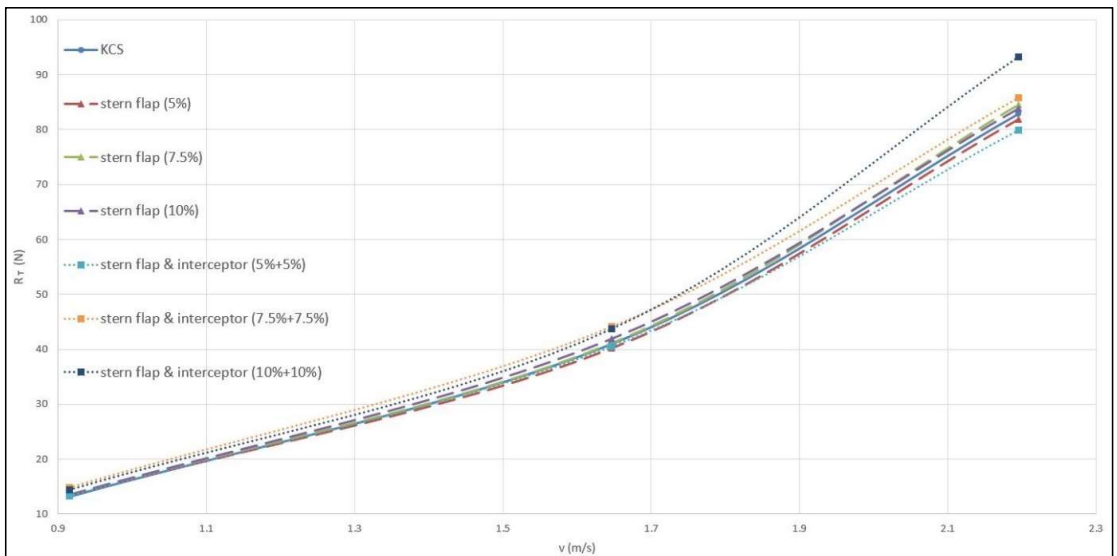


Figure 12. Total resistance values (R_T) of all models estimated at speed up to 2.196 m/s

Figure 11 and 12 show that a reduction of total resistances in Model I and II equipped with stern flaps and a combination of stern flaps & interceptors with chord length of 5% T at $v=2.196$ m/s, can be achieved 3 and 4 up to 5%, respectively. The other models indicate an increase of total resistances of 1 up to 12%.

3. Conclusions

This article is aimed to study the high-speed KCS ship through elaborate computational fluid dynamics (CFD) analysis of its model aiming to further reduce total resistance values at high speeds. The validation of the results obtained in these analyses with those of the experiments of the KCS model published in [1], was accomplished as given in Figure 6. After successful conformity of the simulations performed using the commercial software STAR-CCM+, the developed Models I and II having stern flaps and a combination of stern flaps and interceptors, respectively, were analysed in the same manner and the results obtained were compared to each other.

The Models I and II equipped with stern flaps and a combination of stern flaps & interceptors with chord length of 5 % T, respectively, appear to possess considerably better hydrodynamic characteristics than those equipped with stern appendages with other chord lengths and the basic model without any appendages, since they show lower resistance values and turbulence viscosity alongside the model hulls and better propulsive efficiency (Fig. 7-12).

Conclusively, the results of the performed analyses of these models have indicated that the resistance requirements of Model I and II decrease by up to 3 and 4% compared to the basic model, respectively. Based on the results of this research, it was found out that:

- high-speed ships still can have appropriate improvement potential in total resistance by means of the stern appendages,
- the appendages are suitable for fitting and/or retrofitting with low conversion efforts,
- they can be maintained and repaired with reasonable costs.

References

- [1] Larsson, L., Stern, F., & Visonneau, M. (Eds.). (2013). Numerical ship hydrodynamics: An assessment of the Gothenburg 2010 Workshop. Springer Science & Business Media.
- [2] Avcı, A.G., Barlas, B., Ölçer, A.İ. (2017). An Investigation of Fuel Efficiency in High Speed Vessels by Using Interceptors, International Conference on Maritime Energy Management, World Maritime University, Malmö, Sweden, 24-25 January.
- [3] Zou, J., Lu, S., Jiang, Y., Sun, H., Li, Z. (2019). Experimental and Numerical Research on the Influence of Stern Flap Mounting Angle on Double-Stepped Planing Hull Hydrodynamic Performance, J. Mar. Sci. Eng. 2019, 7, 346.
- [4] Uithof, K., Bouckaert, B., Van Oossanen, P.G., Moerke, N. (2016). The Effects of the Hull Vane On Ship Motions of Ferries and Ropax Vessels, Design & Operation of Ferries & Ro-Pax Vessels, 25-26 May 2016, London, UK.
- [5] Uithof, K., Hagemester, N., Bouckaert, B., Van Oossanen, P.G., Moerke, N. (2017). "A Systematic Comparison of the Influence of the Hull Vane®, Interceptors, Trim Wedges and Ballasting on the Performance of the 50m AMECRC Series #13 Patrol Vessel" International Naval Engineering Conference, Asia 2017, Singapore.
- [6] Cumming, D., Pallard, R., Thornhill, E., Hally, D., Dervin (2006). Hydrodynamic Design of a Stern Flap Appendage for the HALIFAX Class Frigates, MARI-TECH 2006, Halifax, N.S June 14 – 16, 2006.
- [7] Cusanelli, D.S. (2002). "Scaling Effects on Stern Flap Performance Predictions - Progress Report", NSWCCD-50-TR-2002/001
- [8] Avcı, A.G., Barlas, B., (2019). An Experimental Investigation of Interceptors for a High Speed Hull, International Journal of Naval Architecture and Ocean Engineering 11 (2019) 256-273.
- [9] Song, K.W., Guo, C.Y., Gong, J., Li, P., Wang, L.Z., (2018). Influence of Interceptors, Stern Flaps, and their Combinations on the Hydrodynamic Performance of a Deep-Vee Ship, Ocean

Engineering 170, 306–320.

[10] http://www.simman2008.dk/KCS/kcs_geometry.htm (Date of Access: 13.05.2020)

[11] Jongen, T. 1998. “Simulation and Modelling of Turbulent Incompressible Flows”, Ph.D. Thesis, Lausanne EPFL.